Effects of Atmosphere Composition on Soldering Performance of Lead-free Alternatives

C. Christine Dong
Alexander Schwarz
and Dean V. Roth
Air Products and Chemicals Inc.
7201 Hamilton Boulevard
Allentown, PA 18195-1501

Abstract

An experimental study was conducted to evaluate and understand the effects of atmosphere composition on soldering performance of six tin-based, lead-free solders. The performances of each solder were evaluated in terms of 1) oxidation of molten solder in air, 2)dissolution of solder oxides in nitrogen, and 3) reduction of solder oxides in hydrogen and compared with that of eutectic tin-lead solder.

Introduction

Due to environmental and health concerns about lead contamination, there is a strong likelihood of legislation that requires the elimination of lead from electronics manufacturing. Therefore, the soldering industry has made substantial efforts in the past several years searching for viable, lead-free alternatives. This material search is based on several considerations, including: 1) cost and availability, 2) reliability (mechanical, thermal, and electrical properties), and 3) manufacturability (melting point, solderability, and sensitivity to atmosphere).

Although manufacturability is a principal concern in searching for lead-free alternatives, it is still largely unknown at the present time for a lot of newly emerged lead-free solders. A solder that possesses good manufacturability is regarded as having a relatively large and fast solder spread in a suitable temperature range with less sensitivity to oxygen concentration in the soldering atmosphere. Another interesting factor of the manufacturability of a solder is its feasibility for fluxless soldering in a controlled atmosphere. Therefore, our study was aimed at evaluating and understanding the effect of atmosphere composition on soldering performance of lead-free alternatives.

The atmospheres used in this study were air (oxidizing), nitrogen (inert), and hydrogen (reducing). It is understood that the soldering performance of a solder is largely controlled by the extent of solder oxidation. In this study, the performances of each solder were evaluated in terms of 1) oxidation of molten solder in air, 2) dissolution of solder oxides in nitrogen, and 3) reduction of solder oxides in hydrogen. Since most of the newly emerged lead-free solders are based on a ternary or quaternary addition to a tin-based binary system, for the initial study six commonly involved binary lead-free solder systems were selected and compared with eutectic tin-lead solder. The composition and melt-ing point of each solder alloy involved in this study are listed in **Table 1**.

Table 1: Composition and Melting Point of Solder Alloys

Solder	Composition (%)	Melting Point (°C)*
eutectic tin-lead	63Sn/37Pb	183
eutectic tin-silver	96.5Sn/3.5Ag	221
eutectic tin-copper	99.3Sn/0.7Cu	227
peritectic tin-antimony	95Sn/5Sb	240
eutectic tin-bismuth	43Sn/57Bi	138
eutectic tin-indium	48Sn/52In	117
eutectic tin-zinc	91Sn/9Zn	199

*Data are based on International Tin Research Institute (ITRI) internal reports.

Experiments and Discussions

The experimental setup used in this study is shown schematically in **Figure 1**. A quartz tube (2" diameter and 12" long) is mounted in a split furnace with a six-inch heating zone in which a temperature rise similar to that in an IR (infrared) reflow soldering furnace can be obtained. To observe and photograph the liquid solder drop, each end of the quartz tube is sealed with an optical-flat glass, and a light source and a video system are mounted at opposite ends of the tube, respectively. During each heating cycle, the desired soldering atmosphere is maintained by passing gas through the tube with a con-stant gas flow rate of 1.8 liter/minute.

To compare the intrinsic properties of each solder without the influence of fluxes, the fluxless solder preforms (2 mm diameter and 1 mm thick) of each alloy except eutectic tin-bismuth were used in our study. Since eutectic tin-bismuth is very brittle and its preform is not available commercially, fluxless solder wire was employed as an alternative for some experiments.

Oxidation of Molten Solder in Air

Oxidation rate of a molten solder in an oxygen-containing atmosphere is an important characteristic of the solder's manufacturability. In wave soldering, a rapid oxidation of a molten solder will result in a large amount of dross formation, which not only increases the consuming rate of the solder, but also requires more time for system maintenance. For soldering with no-clean technology, the oxidation tendency of a solder becomes a more important issue in comparison with the traditional soldering using RMA fluxes, since the low activity of no-clean fluxes may not be able to

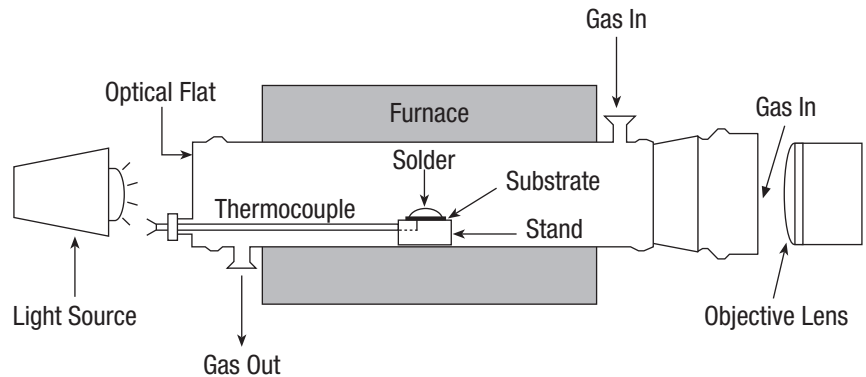Figure 1: Schematic illustration of the experimental setup.

Table 2: Thickness and Composition of Solder Oxides

Solder	Oxide Thickness	(angstrom)*	Dominant Type of Oxide
	10 min	50 min	
63Sn/37Pb	50	500	tin oxides
96.5Sn/3.5Ag	50	50	tin oxides
99.3Sn/0.7Cu	50	50	tin oxides
95Sn/5Sb	875	1425	tin oxides
43Sn/57Bi	350	800	tin oxides
48Sn/52In	175	600	indium oxides
91Sn/9Zn	200	325	zinc oxides

*The experimental error is estimated to be ±10 angstrom.

remove thick solder oxides and thus reduce solderability.

Oxidation rates of molten solders at an equivalent temperature superheat under normal air flow were investigated. Each fluxless solder preform was heated in the tube furnace from room temperature to 500°C in nitrogen and held at this temperature under a hydrogen flow for 10 minutes to remove initial oxides.

The sample inside the tube furnace was then cooled under a nitrogen flow to a temperature that is 140°C above the solder's melting point (m.p.). When the furnace temperature became equilibrated, nitrogen flow was switched to air flow and the sample was held at this temperature for a desired period, such as 10 or 50 minutes. Finally, the furnace was cooled in nitrogen to room temperature. The high temperature (m.p. + 140°C) and the long heating time (10 or 50 min.) were used here to better demonstrate the

difference in oxidation rates among all solders tested and to minimize experimental error. After this oxidation treatment, the thickness and the type of the oxide films formed on each solder were determined using Auger Electron Spectroscopy (AES). The thickness of each oxide film was determined according to half-maximum intensity of oxygen.

The determined oxide film thickness and the type of oxide are summarized in **Table 2**. The dominant type of oxide determined using AES is quite consistent with that predicted based on thermodynamics. According to thermodynamics, an element of a liquid alloy having a lower (or more negative) free energy of oxide formation should migrate to the liquid surface to form oxides. The free energies of oxide formation of all elements involved in this study (Sn, Pb, Ag, Cu, Sb, Bi, In, and Zn) are listed in **Table 3** (Ref. 1). It can be seen that the free energies

of forming indium and zinc oxides are smaller than that of forming tin monoxide. Consequently, in tin-based solders both indium and zinc form oxides more readily than tin, as has been observed. On the other hand, the free energies of oxide formation of other elements (Pb, Ag, Cu, Sb, and Bi) are larger than that of tin, and therefore tin is preferentially oxidized in the solders containing these elements.

Figure 2 shows the oxide thickness as a function of oxidation time. In general, the oxidation tendencies of 95Sn/5Sb, 43Sn/57Bi, 48Sn/52In, and 91Sn/9Zn are all higher than that of 63Sn/37Pb. In contrast, 96.5Sn/3.5Ag and 99.3Sn/0.7Cu exhibit a greater resistance to oxidation as compared to 63Sn/37Pb.

Considering oxidation kinetics, it can be seen from Figure 2 that both 63Sn/37Pb and 48Sn/52In exhibit relatively linear oxidation rates. Normally, a linear oxidation results from the formation of a porous or cracked scale that does not act as a diffusion barrier between the two reactants. In this case, intrinsic chemical reaction controls the total reaction rate. As shown in Table 2, the tin-indium forms indium oxides, and the tin-lead forms tin oxides. It appears that the intrinsic oxidation rate of indium is faster than that of tin.

Figure 2 also shows that both 95Sn/5Sb and 43Sn/57Bi have a nearly parabolic oxidation rate (i.e., the square of an oxide thickness is proportional to oxidation time). In general, reaction rates of a parabolic nature are typical of diffusion-controlled reactions and are usually associated with thick and coherent oxides. In contrast, the oxidation rates of 96.5Sn/3.5Ag and 99.3Sn/0.7Cu are very slow (a similar oxidation rate in Figure 2) and appear to follow a logarithmic rate law (i.e., a limiting oxide thickness is reached). The exact mecha-

Table 3: Free Energy of Formation of Metal Oxides

Element	Common Oxide	Free Energy (Kcal/gram atom oxygen)	
		298K	500K
Sn	SnO	−62	−59
Pb	PbO	−45	−43
Ag	Ag_2O	−2.6	—
Cu	Cu_2O	−35	−31
Sb	Sb_2O_3	−50	−46
Bi	Bi_2O_3	−40	−35
In	In_2O_3	−66	−61
Zn	ZnO	−76	−71

Figure 2: Oxide thickness versus oxidation time for the seven solders evaluated. Each solder was oxidized in air at a temperature that is 140°C above its melting point.
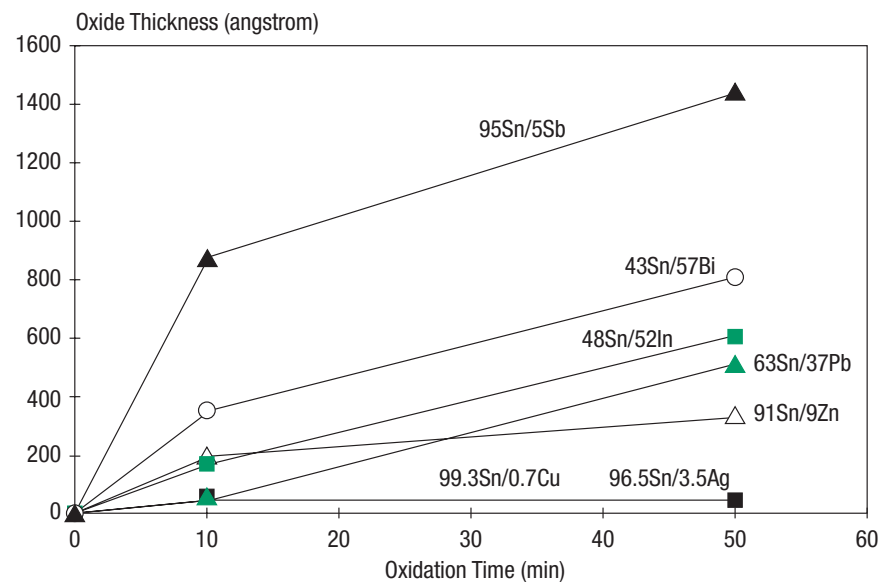
nism of a logarithmic rate behavior is not completely understood yet, but it appears to be a modification of diffusion-limited scale formation. The four solders mentioned above all form tin oxides in which SnO is assumed to be dominant over SnO_2 (Ref. 2). The difference in oxidation rates among the four solders can probably be explained as follows. SnO is a metal-deficient oxide with an excess of tin vacancies (Ref. 3), and the diffusion of tin in the oxide film that takes place through the vacancy mechanism (Ref. 4) is considered to be the controlling step for oxidation. According to Hauffe's valency rule (Ref. 5), for an oxide containing cation vacancies such as SnO, introduction of cations with a higher valence than the solvent

metal, such as Sb^{+3} or Bi^{+3}, increases the vacancy concentration and thus increases oxidation rate of a diffusion-controlled process. On the other hand, the addition of a cation with lower valence, such as Cu^{+1} or Ag^{+1}, decreases the vacancy concentration, resulting in a reduced, diffusion-controlled oxidation rate.

As shown in Figure 2, the oxidation behav-ior of 91Sn/9Zn also follows a logarithmic nature. The oxidation rate of 91Sn/9Zn is relatively fast at the early stage of oxidation, but apparently stops after a period of time. The dominant oxide formed on 91Sn/9Zn is assumed to be ZnO. ZnO, a metal excess oxide (Ref. 6), is relatively dense and can act as a diffusion barrier after reaching certain thickness.

Dissolution of Initial Solder Oxides in Nitrogen

Our previous study (Ref. 7) demonstrated that when a tin-lead solder was heated in nitrogen to a temperature above its melting point, a dissolution of initial surface oxides into bulk liquid solder occurred. The solubility of oxides in molten solder was found to increase with increasing temperature. This phenomenon implies that under certain conditions fluxless soldering may be possible even in an inert soldering environment, and the solderability may be improved simply by increasing soldering temperature. However, the applicability of this inert fluxless soldering depends on the thickness of initial solder oxides and the temperature required to dissolve the oxides.

The thickness of initial oxide film formed on each solder was determined by AES. As shown in **Table 4**, the initial oxide layer on tin-zinc is very thick, about 70 angstrom, while the initial oxide layers on other solders are only about 20 to 30 angstrom.

As shown in **Figure 3**, a molten solder with an initial oxide layer present on its surface tends to maintain its initial solid shape because the thick oxide layer formed on the surface of the solder prevents liquid flow underneath it. However, a molten drop with an oxide-free surface normally forms a nearly spherical shape driven by liquid surface tension. This shape characteristic was used in our study to investigate the temperature required to dis-solve initial oxides on each solder.

A fluxless solder preform was placed on a glass slide, heated in nitrogen (O_2 concentration is about 10 ppm) from room temperature to a temperature above the solder's melting point, and then held at this temperature to ob-
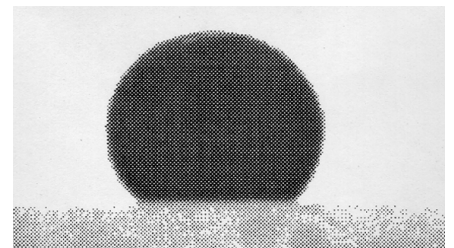
Table 4: Thickness of Initial Oxide Film

Solder	Oxide Thickness (angstrom)
63Sn/37Pb	30
96.5Sn/3.5Ag	30
99.3Sn/0.7Cu	20
95Sn/5Sb	20
43Sn/57Bi	–
48Sn/52In	20
91Sn/9Zn	70

Figure 3: Photographs showing the shape change of a fluxless molten solder when the initial oxide layer is dissolved on heating, (a) before and (b) after the dissolution of the initial oxide layer on heating.
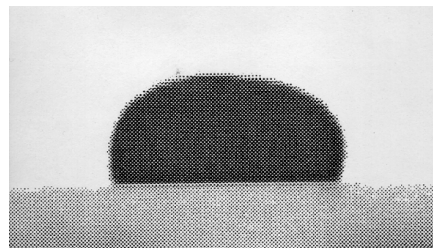
(a)

(b)

serve if there was any shape change on the molten solder. If there was no shape change, the temperature was further increased until a critical temperature was reached, above which the molten solder changed from its initial oxidized shape to a nearly spherical shape. The difference between the critical temperature and the melting point of a solder is defined as temperature superheat to dissolve the initial oxides. The temperature superheats of all solders investigated are summarized in **Table 5**.

As shown in **Table 5**, the thick oxides present on the surface of 91Sn/9Zn could not be completely dissolved by heating in nitrogen. Oxides on surfaces of 96.5Sn/3.5Ag, 99.3Sn/0.7Cu, and 95Sn/5Sb could be easily dissolved, and the temperature superheats were below 20°C. However, the temperature superheats to dissolve oxides of 48Sn/52In and 63Sn/37Pb were relatively high (>77°C).

This result suggests that the temperature superheats for reflow of 96.5Sn/3.5Ag, 99.3Sn/0.7Cu, and

95Sn/5Sb in nitrogen can be lower than that of 63Sn/37Pb. To further prove this, the spread temperature of each fluxless solder preform on a Au/Ni-coated copper plate was determined under nitrogen environments with O_2 concentration ranging from 10 to 10,000 ppm. The Au/Ni-coated copper is relatively immune to oxidation and thus can provide a wettable surface. It can be seen in **Table 6** that the temperature superheats for reflow of 96.5Sn/3.5Ag, 99.3Sn/0.7Cu, and 95Sn/5Sb are significantly lower and less sensitive to O_2 impurity level than that of 63Sn/37Pb.

Reduction of Solder Oxides in Hydrogen

Fluxless soldering using a reducing gas such as hydrogen is always desired because it can eliminate post-cleaning and the possibility of introducing flux residues. Whether or not an oxide can be reduced by hydrogen depends on the stability of the oxide at the given temperature and hydrogen/water partial pres-

sure. However, the reduction rate can be extremely slow even when the oxide is thermodynamically unstable, which makes the reduction process practically ineffective (Refs. 8 and 9). This ineffectiveness of hydrogen is attributed to the lack of reactivity of the hydrogen molecule at low temperatures. It is believed that highly reactive radicals, such as mon-atomic hydrogen, form at higher temperatures (Ref. 10). Therefore, an initiation temperature should exist for each solder above which the reduction rate of solder oxides is acceptable for a normal soldering process.

To find the initiation temperature, isothermal reduction rates of solder oxides on each solder at various temperatures were investigated in this study. The reduction rate was determined by observing the rate of the shape change of a preoxidized fluxless solder preform on glass at a given temperature when exposed to hydrogen. A thick initial oxide layer on the surface of each solder preform is desirable for this study because it minimizes the dissolution effect of solder oxides and makes the shape change more distinguishable. To develop a thick oxide layer, each solder preform was preoxidized by heating up in air from room temperature to a temperature that is 140°C above its melting point and cooling to room temperature in nitrogen. After this preoxidation, the thickness of each oxide layer present was determined by AES. The preoxidized preforms were placed on glass slides and heated in nitrogen to various temperatures, and then the nitrogen flow was switched to a hydrogen flow after the temperature was stabilized. As soon as the hydrogen flow was introduced, the shape of the molten solder was monitored in situ, and the time needed for the molten solder to change from its initial oxidized shape to a stable final shape was recorded. An average reduction rate can be obtained from the ratio

of the initial oxide thickness over the reduction period.

The obtained reduction rate of solder oxides on each solder is plotted in **Figure 4** as a function of temperature. It can be seen that the reduction rate for each type of oxide is very low at low temperatures and increases with increasing temperature in an accelerative way.

This reduction behavior suggests a surface reaction-controlled reduction process because a chemical step is usually much more temperature-sensitive than physical steps. When the surface reaction is the rate controlling step, the isothermal reduction rate, v, can be expressed as :

$$v = k' \exp(- Q/RT) \, C_O \, P_{H2}/RT$$

where k' is the velocity constant, Q represents the activation energy, R is

the gas constant, T is absolute temperature, C_O stands for the concentration of surface oxygen site, and P_{H2} is the partial pressure of hydrogen. Therefore, each reduction rate increases almost exponentially with increasing temperature.

In a normal soldering process, the thickness of the initial oxide layers on a solder joint ranges from 20 to 30 angstrom and the reflow time is about 1 to 1.5 minutes. In this case, the reduction rate of solder oxides must exceed 20 angstrom per minute to ensure solderability. If we assume that a reduction rate of 20 angstrom per minute is acceptable, the initiation temperature for hydrogen to effectively reduce solder oxides on each solder can be found. As shown in Table 7, zinc oxides on the surface of 91Sn/9Zn are the most difficult ones to reduce. The initiation temperature

Table 5: Temperature and Temperature Superheat in N$_2$ for Dissolving

Solder	Melting Point (°C)	Temperature for Dissolving Oxides* (°C)	Superheat* (°C)
63Sn/37Pb	183	~260	~77
96.5Sn/3.5Ag	221	~240	~19
99.3Sn/0.7Cu	227	~245	~18
95Sn/5Sb	240	~250	~10
43Sn/57Bi	138	—	—
48Sn/52In	117	~210	~93
91Sn/9Zn	199	>500**	>301**

*The experimental error is ±5°C.
**The highest temperature used in the experiment was 500°C.

Table 6: Temperature and Temperature Superheat in N$_2$ for Solder Spread

Solder	Melting Point (°C)	Spread Temperature (°C)* 10ppm	100ppm	1000ppm	10,000ppm	Superheat (°C)*
63Sn/37Pb	183	205	207	270	ns	22–87 (O$_2$ ≤ 1000 ppm)
96.5Sn/3.5Ag	221	230	238	240	ns	9–19 (O$_2$ ≤ 1000 ppm)
99.3Sn/0.7Cu	227	230	234	245	ns	3–18 (O$_2$ ≤ 1000 ppm)
95Sn/5Sb	240	246	255	258	ns	6–18 (O$_2$ ≤ 1000 ppm)
43Sn/57Bi	138	—	—	—	—	—
48Sn/52In	117	200	ns	ns	ns	83 (O$_2$ ≤ 10 ppm)
91Sn/9Zn	199	ns	ns	ns	ns	not exist

*The experimental error is ±3°C.
ns: The solder did not spread at the indicated O$_2$ impurity level.

is as high as 510°C. To reduce indium oxides on 48Sn/52In, the initiation temperature is around 470°C. The initiation temperature to reduce tin oxides on 63Sn/37Pb, 96.5Sn/3.5Ag, 99.3Sn/0.7Cu, and 95Sn/5Sb, however, is only 430°C.

The difference in the initiation temperatures among the solder oxides involved is believed to be related to the metal-oxygen bond strength (or heat of oxide formation) of each oxide. The higher the strength of a metal-oxygen bond (or the lower the heat of oxide formation), the higher the initiation tem-perature should be (Ref. 11). Comparing **Table 7** with **Table 8** (Ref. 1), this relationship between initiation temperature and bond strength is demonstrated.

It should be pointed out that the reduction rate and the initiation temperature are functions of not only solder alloy but also the size of solder. A tiny solder drop, such as a solder bump of 40μm in size used in flip chip technology, has a relatively high surface-to-volume ratio and thus possesses a large thermodynamic driving force for surface reduction. Therefore, the reduction rate of solder oxides on such small solder drop can be much higher and the initiation temperature can be significantly lower than that determined here (Ref. 7).

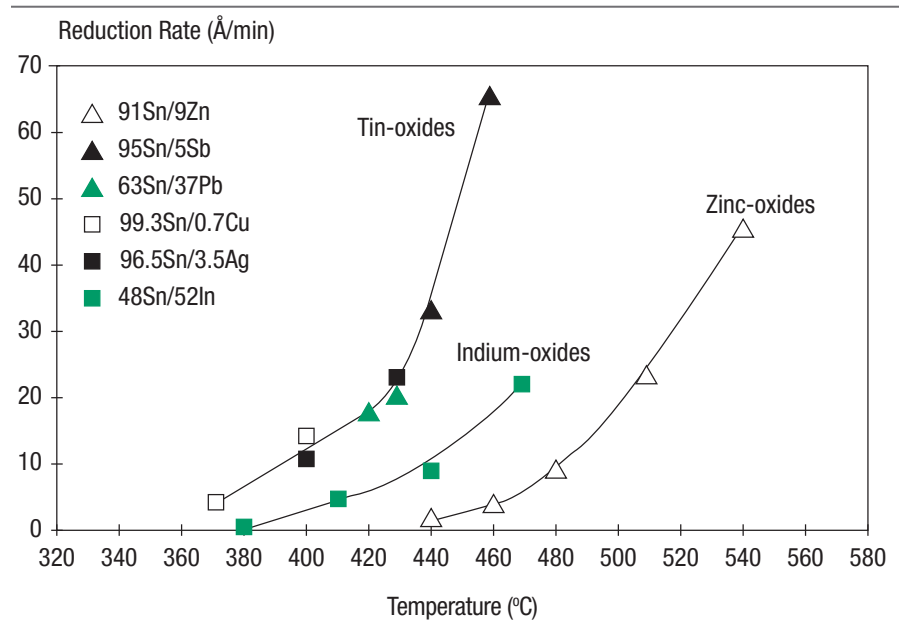**Figure 4: Reduction rate of solder oxides on each solder as a function of temperature.**

Table 7: Initiation Temperature for Hydrogen to Reduce Solder Oxides

Solder	Dominant Type of Oxide	Initiation Temperature (°C)*
63Sn/37Pb	tin oxides	~430
96.5Sn/3.5Ag	tin oxides	~430
99.3Sn/0.7Cu	tin oxides	~430
95Sn/5Sb	tin oxides	~430
43Sn/57Bi	tin oxides	—
48Sn/52In	indium oxides	~470
91Sn/9Zn	zinc oxides	~510

*The experimental error is ±5°C.

Table 8: Heats for Formation of Oxides

Oxide	Heat (Kcal/gram atom oxygen)
SnO	−68.4
In_2O_3	−74.2
ZnO	−83.2

Conclusions

The performances of lead-free and eutectic tin-lead solders have been evaluated for different soldering environments, specifically, oxidation of molten solder in air, dissolution of solder oxides in nitrogen, and reduction of solder oxides in hydrogen. The major conclusions of this study are summarized as follows.

1. Under oxidizing conditions, elements of liquid solder having a lower (or more negative) free energy of oxide formation are oxidized preferentially at the surface of the solder.

2. The oxidation tendencies of 95Sn/5Sb, 43Sn/57Bi, 48Sn/52In, and 91Sn/9Zn are all higher than that of eutectic tin-lead solder. In contrast, both 96.5Sn/3.5Ag and 99.3Sn/0.7Cu have greater resistance to oxidation as compared to 63Sn/37Pb. The difference in oxidation rates of form-ing tin oxides on 95Sn/5Sb, 43Sn/57Bi, 96.5Sn/3.5Ag, and 99.3Sn/0.7Cu follows Hauffe's valency rule.

3. There is a natural dissolution of initial surface oxides into bulk liquid solder at high temperatures under nitrogen flow. The temperature superheats required for dissolving initial oxides and for reflow of 96.5Sn/3.5Ag, 99.3Sn/0.7Cu, and 95Sn/5Sb in nitrogen are lower than that of 63Sn/37Pb.

4. The initiation temperatures for hydrogen to reduce zinc oxides, indium oxides, and tin oxides are 510oC, 470oC, and 430°C, respectively; therefore, it is more difficult to employ fluxless soldering by using tin-zinc and tin-indium solders as compared to eutectic tin-lead solder.

Acknowledgments

References

1. R. C. Weast, Handbook of Chemistry and Physics, 57th edition, CRC press, Ohio, U. S., (1976–1977).

2. D. M. Tench, M. W. Kendig, D. P. Anderson, D.D. Hillman, G. K. Lucey, and J. Gher, "Production Validation of SERA Solder-ability Test Method," Soldering & Surface Mount Technology, 13 46–50 (1993).

3. R. J. Klein Wassink, Soldering in Electron-ics, 2nd Edition, Electrochemical Publica-tion Limited, 8 Barns St., Ayr, Scotland, 221 (1989).

4. R. E. Reed-Hill, Physical Metallurgy Prin-ciples, 2nd Edition, Brooks/Cole Engineering Division, Monterey, California, U.S., 386–390 (1973).

5. K. Hauffe, Progr. Metal Phys., 4 71 (1953).

6 W. D. Kingery, H. K. Bowen, and D. R. Uhl-mann, Introduction to Ceramics, 2nd Edi-tion, John Wiley & Sons, Inc., N.Y., U.S., 241 (1976).

7 C. C. Dong, G. K. Arslanian, and Rao Bonda, "Fluxless Soldering of Flip Chip Assemblies," Nepcon West '96, Proceed-ings of the technical Program, 96–110 (1996).

8 R. D. Deshmukh, M. F. Brady, R. A. Roll, and L. A. King, "Active Atmosphere Solder Self-Alignment and Bonding of Optical Components," The International Journal of Microcircuits and Electronic Packaging, 16 [2] 97–107 (1993).

9 B. Ozturk, P. Barron, and R. J. Fruehan, "Physical Chemistry of Gas Liquid Solder Reactions," Metallurgical Transactions B, 18B 577-582 (1987).

10 G. Wang and D. Hauser, "State of the Art in Fluxless Soldering," EWI, 3 (1995).

11 W. A. Oates and D. D. Todd, "Kinetics of the Reduction of Oxides," The Journal of the Australian Institute of Metals, 7 [2] 109–114 (1962).

· ·

**For more information,
please contact us at:**

Corporate Headquarters
Air Products and Chemicals, Inc. 7201 Hamilton Boulevard Allentown, PA 18195-1501
T 800-654-4567
T 610-706-4730
F 800-272-4449
F 610-706-6890
gigmrktg@airproducts.com

Regional Head Offices
Air Products PLC
Hersham Place Technology Park
Molesey Road
Walton-on-Thames
Surrey KT12 4RZ
UK
T +44-0-1270-614314
apbulkuk@airproducts.com

Air Products Asia, Inc.
2 International Business Park #03-32
The Strategy Singapore 609930
T +65-6494-2240
F +65-6334-1005
sgpinfo@airproducts.com

AIR PRODUCTS

tell me more
airproducts.com/Industries/Electronics-Assembly